Casing Vibration and Gas Turbine Operating Conditions

K. Mathioudakis
Lecturer.

E. Loukis
Research Assistant.

K. D. Papailiou
Professor.

National Technical University of Athens,
Laboratory of Thermal Turbomachines,
15710 Athens, Greece

The results from an experimental investigation of the compressor casing vibration of an industrial gas turbine are presented. It is demonstrated that statistical properties of acceleration signals can be linked with engine operating conditions. The power content of such signals is dominated by contributions originating from the stages of the compressor, while the contribution of the shaft excitation is secondary. Using nonparametric identification methods, accelerometer outputs are correlated to unsteady pressure measurements taken by fast response transducers at the inner surface of the compressor casing. The transfer functions allow reconstruction of unsteady pressure signal features from the accelerometer readings. A possibility is thus provided for "seeing" the unsteady pressure field of the rotor blades without actually penetrating through the casing, but by simply observing its external surface vibrations.

1 Introduction

Recognition of the benefits from gas turbine condition monitoring has led to a rapid growth of related systems and techniques in recent years. Both gas path analysis and vibration techniques are in use. Vibration monitoring in particular provides important information about machinery health, as it can reveal the cause of potential problems and provide an early indication of incipient mechanical failures. This gives the possibility for diagnosing and correcting malfunctions, leading to an optimum management of engine operation with respect to engine shutdown and maintenance. In order to fulfill this purpose, before setting up a vibration monitoring system, the following items have to be studied:

- Selection of engine parts to be covered by the system and appropriate measuring locations.
- Measuring instruments to be used.
- Data evaluation procedures and criteria for deciding on the significance of collected data.
- Vibration limits and reference values that establish the condition of an engine.

A basis for selecting and justifying a vibration monitoring system has been provided in a recent paper (Lifson et al., 1989), where a number of case histories has also been presented. A discussion of vibration limits and vibration sources has been provided by Lifshits et al. (1986), while aspects of data evaluation and interpretation have been covered by Baines (1987), Bently et al. (1986), and Laws and Muszynska (1987). These authors also give an overview of recent progress in the area.

The aspects of malfunction covered in most of the recent publications refer mainly to problems showing up in shaft-related vibrations (the test cases presented by the abovementioned authors). Such problems are, for example, bearing failures, misalignment, shaft cracks, structural resonances, unbalance, shaft bow, fluid film and bearing instability, rubs, etc. Most of the published data and fault signatures discussed in the open literature refer to such cases. Identification of the condition of the blading itself has not received much attention, although blading problems have been reported by Barschdorff and Korthauer (1986) to rank among the most frequent faults. They presented a study related to blading problems and the emphasis was on pattern recognition, applied in identifying blade damages.

The investigation reported in the present paper is focused on studying the vibrational behavior of a gas turbine compressor casing, with respect to engine operating conditions. The purpose is to form a background for fault studies. Before the actual faults are studied, the dependence of casing vibration characteristics on engine operating conditions has to be examined. The reasons for proceeding that way are multiple: first, to understand the nature of sources exciting casing vibration, second, to study their behavior for different operating conditions of a healthy engine (baseline information), and third, to attempt to correlate engine outer surface measurements to events in engine interior. An industrial gas turbine has been used as a test engine.

In the following we start by describing the background reasoning, which leads to the choice of the particular measurements and the procedure we use. The experimental setup, results from the measurements, and conclusions from the data elaboration are given.

2 Background of the Investigation

The investigation was designed as a part of a more general study aiming at the identification of failures of compressor rotor blades, by means of vibration measurements. The measurements had therefore to be chosen in such a way that they are influenced by excitations originating from the rotating

Contributed by the International Gas Turbine Institute and presented at the 34th International Gas Turbine and Aeroengine Congress and Exhibition, Toronto, Ontario, Canada, June 4–8, 1989. Manuscript received at ASME Headquarters January 17, 1989. Paper No. 89-GT-78.

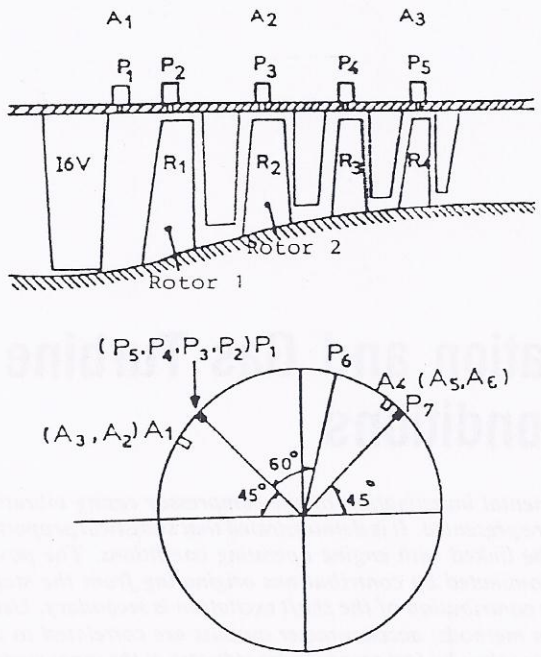

Fig. 1 Positions of pressure transducers and accelerometers on the compressor casing

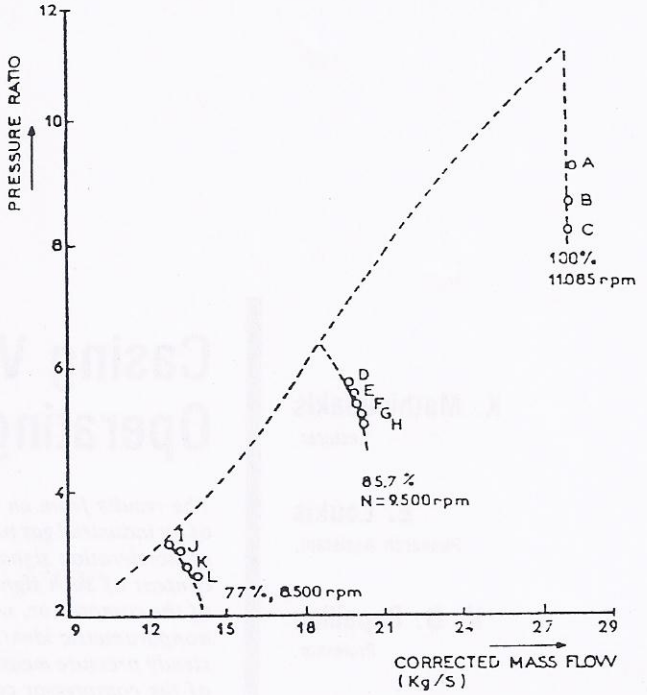

Fig. 2 Operating points for the experiments on the compressor map

blades. Suitable measuring positions for that purpose were chosen at the outer surface of the compressor casing.

The vibration of the casing surface is excited by forces of two kinds: (*a*) forces transmitted through its junctions to the intake and the rear part of the engine. They represent vibrations originating at different engine components, reaching the casing by transmission paths through the engine structure. (*b*) Forces of aerodynamic origin. They are created by (*i*) pressure fields of rotating blade rows, (*ii*) acoustic waves propagating inside the annulus, (*iii*) pressure fluctuations from turbulent flow phenomena, and (*iv*) unsteady forces from stator blades fixed on the casing. For all these forces, the fundamental cause is the rotation of the blade-to-blade pressure fields of rotors. This therefore is considered as the main exciting mechanism, as far as aerodynamic forces are considered.

The pattern of the blade-to-blade pressure field around a rotor circumference depends on the geometric shape of the blades, which reflects their mechanical condition. (It changes when blade faults occur, as for example blade bending, loss, or blade shape changes due to erosion or fouling.) On the other hand the change of the operating condition of a compressor blade row corresponds to a change in the pressure distribution along the blade surface. The casing vibrations are therefore expected to vary with the compressor operating point.

This variation needs to be studied for two main reasons: (*i*) In order to establish baseline information for casing vibration sensors, we should know how their readings vary for various operating points. Such variations are not due to any change in the mechanical conditions of the blades and should therefore be known in order to avoid misinterpretation of related shifts. (*ii*) Since the excitation and the resulting vibration change with the operating point, it will be useful to study how the casing response is influenced. We also want to examine whether a casing transfer function can be established.

In order to establish the relation between casing vibrations and excitations inside the engine, measurements must be performed of both the engine outer casing surface vibration and the internal pressure field. On the other hand, a complete experimental data set covering the entire operating range of the compressor that is as reliable as possible must be acquired.

We describe now the setup and the procedure for the experiments.

3 Experimental Setup and Procedure

The experiments were carried out on the single shaft version of the Tornado Gas Turbine, manufactured by Ruston Gas Turbines, with a nominal output of 6.2 MW at 11,085 rpm. A description of the engine has been given by Wood (1981).

Six accelerometers were mounted on the outer surface of the compressor casing. They were piezoelectric, manufactured by METRAVIB-RDS (model AM-109-MP) with a frequency range 1.5 Hz to 10 kHz, a linearity ±2 percent up to 1000*g*, and a minimum resonant frequency of 30 kHz. Fast response pressure transducers were flush mounted at the compressor inner casing wall. They were Kulite XST-190-25 SG. The positioning of the sensors on the compressor casing is shown schematically in Fig. 1.

Data were acquired through a data acquisition system manufactured by LMS, with a total capacity of 32 channels and maximum total sampling frequency of 960 kHz. A key phasor signal, bearing proximity probe signals from all engine bear-

Nomenclature

a = casing surface acceleration
A_i = accelerometer number i; Fig. 1
[H] = transfer matrix; equation (2)
p = internal casing wall static pressure
P_i = pressure transducer i; Fig. 1
S_{xx} = autospectrum of a system input x
S_{xy} = cross-spectrum of a system input x to an output y
[Y] = column vector consisting of the Fourier transforms Y of outputs y
[X] = column vector consisting of the Fourier transforms X of inputs x

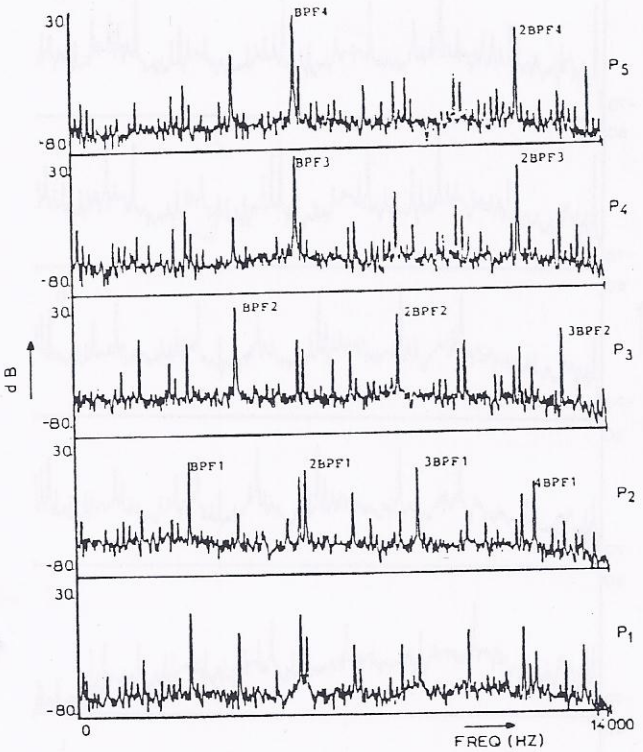

Fig. 3 Power spectra from pressure transducers at operating point F

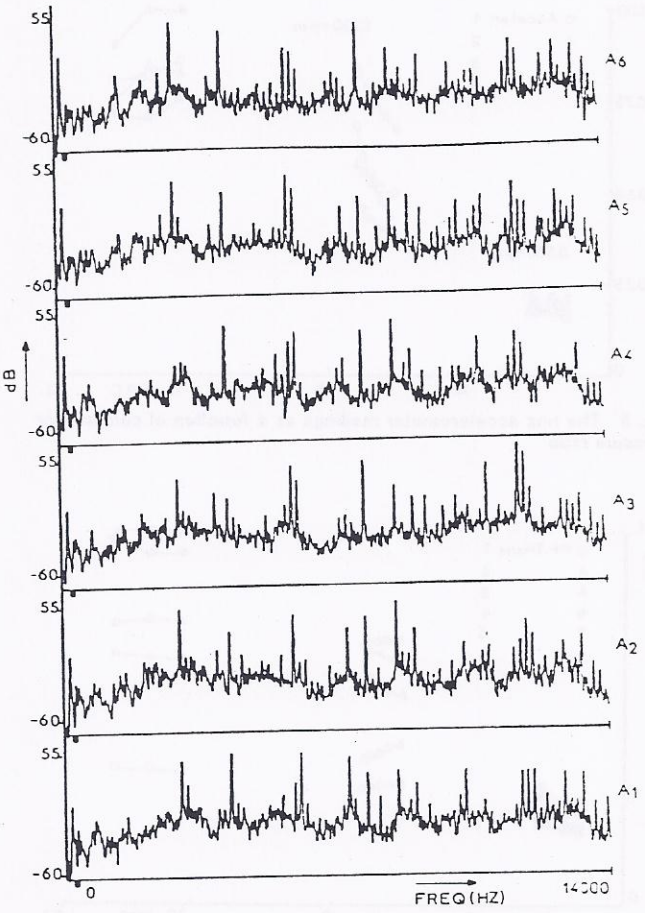

Fig. 4 Power spectra from accelerometers at operating point F

ings, and acoustic signals from microphones placed around the engine, were acquired simultaneously with unsteady pressure and acceleration. Aerodynamic performance data were acquired by means of a data logging system described by Timperley and Smith (1983). Performance data provide information about operating conditions and cycle parameters for each operating point.

The engine operating points at which unsteady measurement data were acquired are shown on the compressor performance map (Carchedi and Wood, 1982) of Fig. 2. The results presented here were derived from data strings of 8192 samples per channel, with acquisition frequencies of 34 kHz (data at 9500 rpm, 11,085 rpm) and 24 kHz (data at 8500 rpm).

4 Accelerometers and Pressure Transducer Signal Features

The results of the measurements of unsteady pressure at the inner surface of the casing and acceleration on the outer surface are now presented. First the power spectra of the signals are discussed, while dependence on operating conditions is discussed afterward. Although only representative results are given here, the discussion is based on observations of the full amount of data.

4.1 Unsteady Pressure. Some sample power spectra of pressure signals are shown in Fig. 3. Since the frequencies excited by the individual rotor blade rows are known (blades/row × frequency of rotation), the relative importance of blade row interactions can be estimated from such spectra. It can be seen that the signal of each pressure transducer facing a rotor blade row is dominated by components with frequencies generated by the corresponding blade row. Harmonics corresponding to rotors of neighboring stages are also present, but they are of much smaller magnitude. This shows that the pressure field generated by a rotating blade row is not strongly influenced by the fields of the rotors of the neighboring stages. The presence of these harmonics, however, shows that they cannot be ignored, if one is interested in interpreting the data or possibly producing a model of the pressure field.

4.2 Accelerometer Signals. The spectra of the six casing accelerometers at the same operating point are shown in Fig. 4. Before commenting on these, it must be pointed out that they extend up to 14 kHz. Attention should be focused however on frequencies up to 10 kHz, since this is the useful range of the accelerometers. It can be noticed that in the spectra of all the accelerometers, peaks of comparable magnitude are present for the frequencies excited by different rotors. Therefore, vibrations measured at an axial location corresponding to a blade row are not necessarily dominated by the excitation of that row, but contain frequencies excited by the blade rows at other axial positions as well. On the other hand the relative importance of the harmonics is different for the different locations on the casing. This is interpreted as a consequence of the asymmetry of the casing geometry, which results in different transmission paths even for accelerometers placed at the same axial position.

These observations coming from a first glance at the signals indicate already that since the accelerometers contain information from adjacent blade rows, a suitable combination of accelerometer signals could be processed in order to derive information about what is happening in each blade row along the compressor.

Inspection of the spectra shows also that the signal energy is contained mainly in the higher frequencies and in particular, in frequencies corresponding to the blade passing of different rotors. Therefore, vibrations transmitted from the shaft through the bearings to the casing are of secondary importance. This picture changes slightly when we examine different operating points.

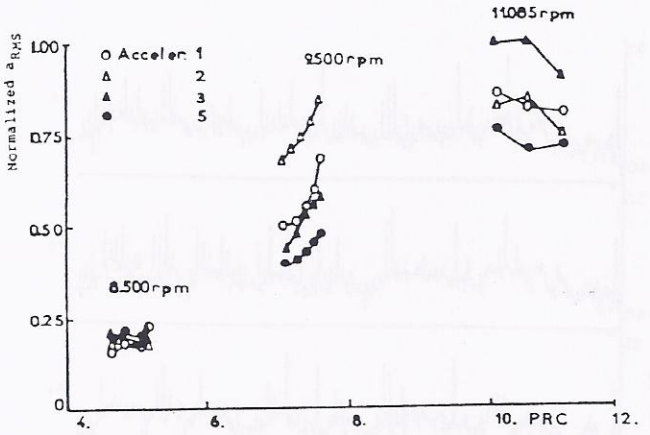

Fig. 5 The rms accelerometer readings as a function of compressor pressure ratio

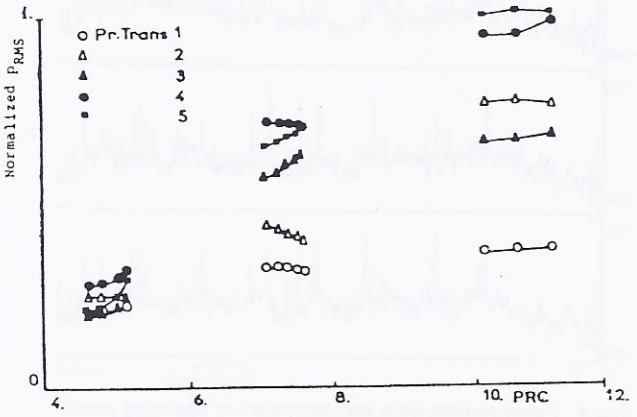

Fig. 6 The rms pressure transducer readings as a function of compressor pressure ratio

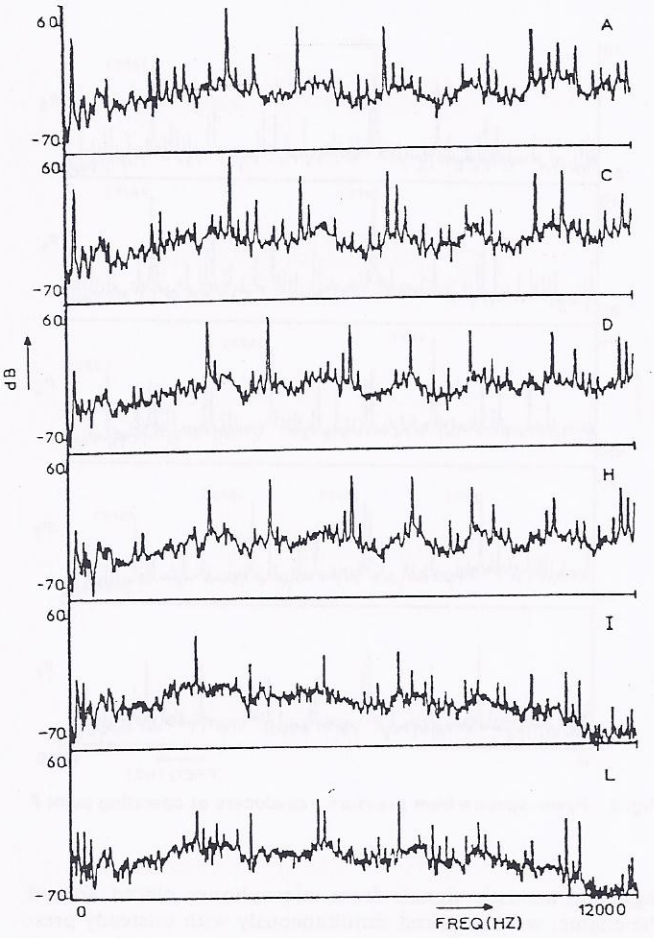

Fig. 7 Power spectra from accelerometer A1 at operating points A, C, D, H, I, and L

This leads to a conclusion about diagnostics: Casing acceleration measurements should be used very carefully when they are meant to detect shaft-related problems. Appropriate filtering should be employed in order to extract excitations from rotating blades, which contribute most of the signal energy.

4.3 Dependence on Operating Conditions. The observation that the accelerometer signals contain information from the excitation of the compressor blade rows suggests that the features of accelerometer signals depend on engine operating point (defined, for example, by rotational speed and output load).

A feature of the signals that we examine in this respect is the rms value, defined as follows:

$$X_{\text{rms}} = \left| \frac{1}{N-1} \sum_{i=1}^{N} (x_i - \bar{x})^2 \right|^{1/2} \quad \text{where } \bar{x} = \frac{1}{N} \sum_{i=1}^{N} x_i \qquad (1)$$

N is the number of points used. This quantity represents the energy content of the signal within the range of frequencies covered. It reflects changes in amplitudes of the different harmonics in a global manner, without showing how the changes are distributed among them. We shall first examine its variation with operating point and we will subsequently proceed in examining how its changes are distributed among individual harmonics.

The rms accelerometer signals for the different operating points of our experiments are shown in Fig. 5. This figure shows the following: (1) The overall level of the rms changes significantly from one speed to another, in comparison to smaller changes on each speedline. (2) At one operating speed the rms is changing with the pressure ratio. The change is monotonous for the cases of 8500 and 9500 rpm.

In order to examine whether the observed changes correspond to a similar behavior of the excitation forces from pressure transducers and bearings, the rms of the corresponding signals has also been examined as a function of the engine operating point.

Figure 6 shows the dependence of pressure transducer rms on operating point. It can be seen that the rms of the unsteady pressure signals is also varying with the operating point. In particular we observe that: (1) Changing the rotational speed gives a drastic increase of values of the rms, in comparison to the changes observed on one speedline. (2) The trends of the change at 8500 and 9500 rpm are monotonous, which is not the case for 11,085 rpm. From this point of view, the trends are similar to those of the accelerometers.

Finally, inspecting the rms values of signals from the bearing proximity probes showed that they do not exhibit a significant variation. These observations indicate that the vibrations of the casing outer surface are directly linked to the internal pressure field.

Further processing of the time domain signals of both the pressure transducers and accelerometers was done. Correlation functions and phase averages have been calculated and their dependence on operating point was examined. Results are not presented here due to space limitations. A conclusion drawn from this processing is that pressure transducer signals are far more suitable than accelerometer signals, for identifying blade

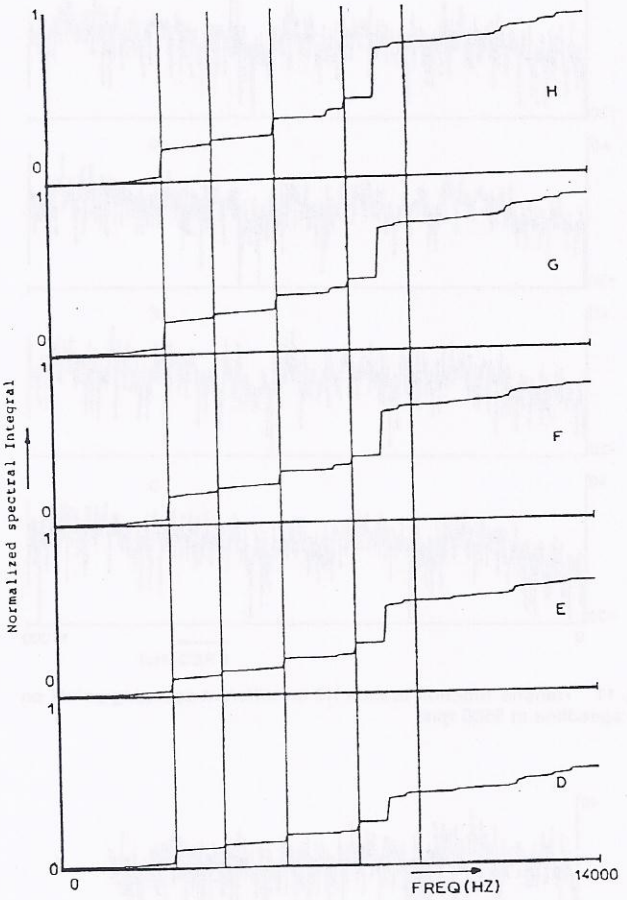

Fig. 8 Energy addition along the frequency range, for operating points D, E, F, G, and H. Accelerometer A2

operating conditions as well as blade faults. More details are given by Mathioudakis et al. (1988).

4.4 Power Spectra for Different Operating Conditions. We will examine now how the spectra change with the engine operating conditions. In Fig. 7 we show power spectra of signals from accelerometer A1 for two operating points on each speedline of Fig. 2. The spectra at one rotational speed show that the pattern of the harmonics remains basically the same, but their relative amplitudes are changing. Spectra at the different rotational speeds contain harmonics at the corresponding frequencies. It must be noted, however, that the "envelope" of the spectrum looks similar, for all these operating conditions.

In order to examine how the signal energy is distributed within the range of frequencies of interest, we integrate the spectra. An example of a result of the integration is shown in Fig. 8. The quantity on the Y axis is the integral of the spectral density from zero to a particular frequency f. This quantity is therefore the energy content of the signal in the frequency range from 0 to f Hz. Observing its evolution along the frequency range, we can see at what frequencies the energy is contained. It is seen that the energy is contained mainly in the frequencies of blade passing of the rotor blade rows, while the broadband contribution is rather minor. This observation confirms our previous comment, that the casing vibration is mainly excited by aerodynamic sources (unsteady pressure field) coming from the compressor interior. On the other hand, the change of the overall energy (equal to the variance) shown in Fig. 6 varies with operating conditions, due to a change of the contributions at the individual rotor blade passing frequencies. In Fig. 8, for example, the change of the total energy content is caused mainly by the change of the contribution of the second harmonic of the rotor 2 blade row.

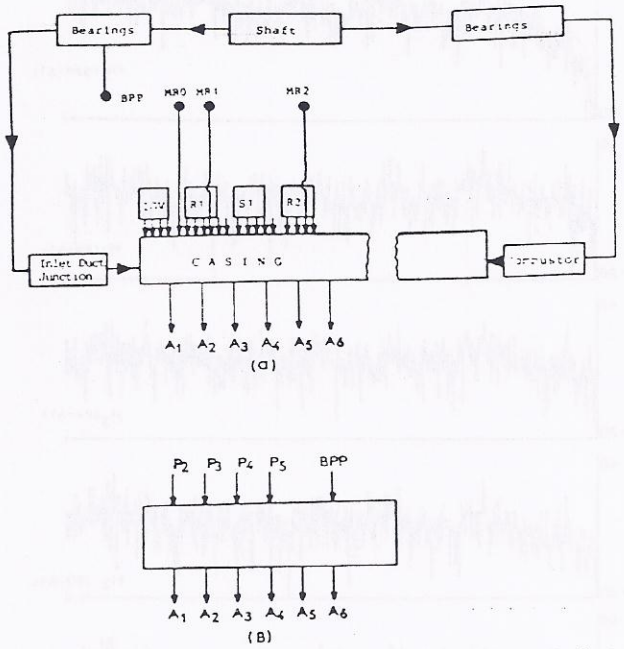

Fig. 9 The compressor casing as a linear system: *(a)* the full, distributed input-output system; *(b)* the lumped input-output system

5 Interrelation Between Unsteady Pressure Field and Acceleration Measurements

Having at our disposal measurements of both the exciting forces and the vibratory responses of the casing, its transmission characteristics can be established. Knowledge of them can be used for diagnostics, since it enables: (*i*) the calculation of the casing vibrations, when the excitations (rotor blade pressure field, associated with either "healthy" or "nonhealthy" engine operation) are known. This gives the possibility of simulating the effects of blade faults. (*ii*) The calculation of the excitations when the response is known, namely the reconstruction of the unsteady pressure signals, from acceleration measurements. This capability is very important from a diagnostics point of view. As we have seen, unsteady pressure signals are far more suitable for determining the stage where a fault or a defect has occurred, since they are influenced mainly by the corresponding blade row.

5.1 Transfer Function Considerations. The transmission characteristics of the compressor casing can be mathematically expressed as a set of vector transfer functions, if the compressor casing is modeled as a linear system.

The inputs of the linear system are all the excitations of the casing. They are continuously distributed over the internal surface of the casing and its connections to adjacent engine components. A schematic view of the system and the excitations is shown in Fig. 9(*a*). It is a distributed parameter, distributed input system. In order to study its characteristics, we lump the most important excitations and form an equivalent system with lumped inputs. The vibration of any point of the compressor casing can be considered as output of the linear system. The resulting simplified system is shown in Fig. 9(*b*).

The calculation of any of the vector transfer functions from time domain signals is based on a well-established method known from systems theory; see for example Bendat and Piersol (1971). The main equation employed is

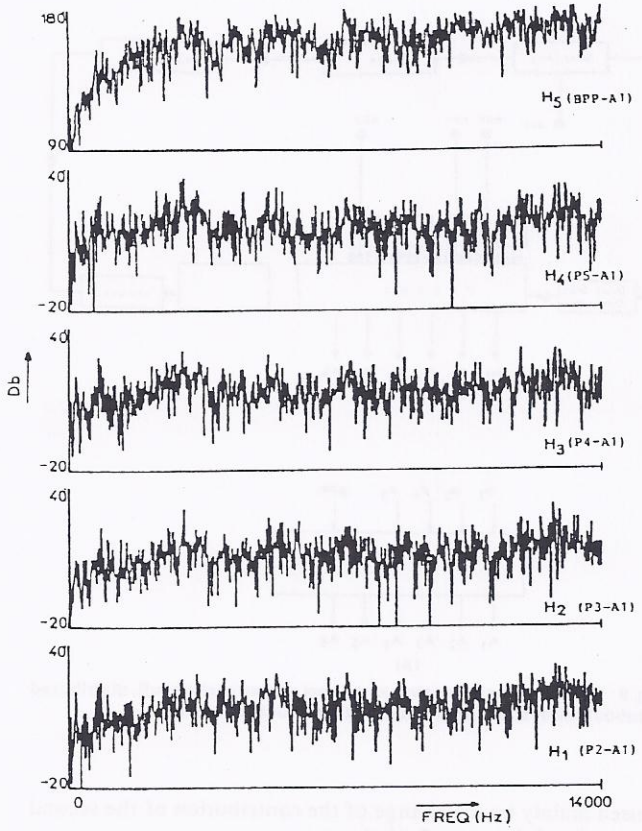

Fig. 10 Amplitudes (in db) of the three transfer function branches between accelerometer A2 and unsteady pressure transducers P2, P3, P4, and P5 and inlet bearing proximity probe: point F

$$[H(f)] = [S_{xy}(f)]^{-1}[S_{xx}(f)] \quad (2)$$

This equation has been implemented together with appropriate averaging procedures, in order to reduce the influence of stochastic noise in the signals (Mathioudakis et al., 1988).

The vector transfer functions are expected to depend on the dynamics of the compressor casing; dependence on operating point is envisaged, only as long as casing temperature variations occur.

Vector transfer functions were calculated from our data, according to the model of Fig. 9(*b*). A representative result is shown in Fig. 10, where we see the transfer function branches for the five inputs and accelerometer A1 as output, for operating point F. During our study we have examined various combinations of inputs and the corresponding transfer functions. The main contributors to a specific output can be determined by discarding some of the inputs and seeing whether significant changes in the result are produced. In this way we have found that the main contributors to each accelerometer are the pressure transducers P2, P3, and P4 (see Fig. 1).

5.2 Dependence on Operating Point. In Fig. 11 we see one branch of the vector transfer functions for operating points H, G, E, and D, which lie on the 9500 rpm speedline. A comparison between them shows that despite small differences, a general similarity exists. This conclusion has been found to be also valid for points on the other two speedlines of 8500 rpm and 11,085 rpm. Since visual inspection or crossplots do not form a proof of similarity, a more rigorous proof for this observation has been given through signal reconstruction, which will be discussed in the next section.

A comparison between corresponding branches for operating points of different speedlines has also been done. In Fig. 12 we can see the results for the operating points J and B,

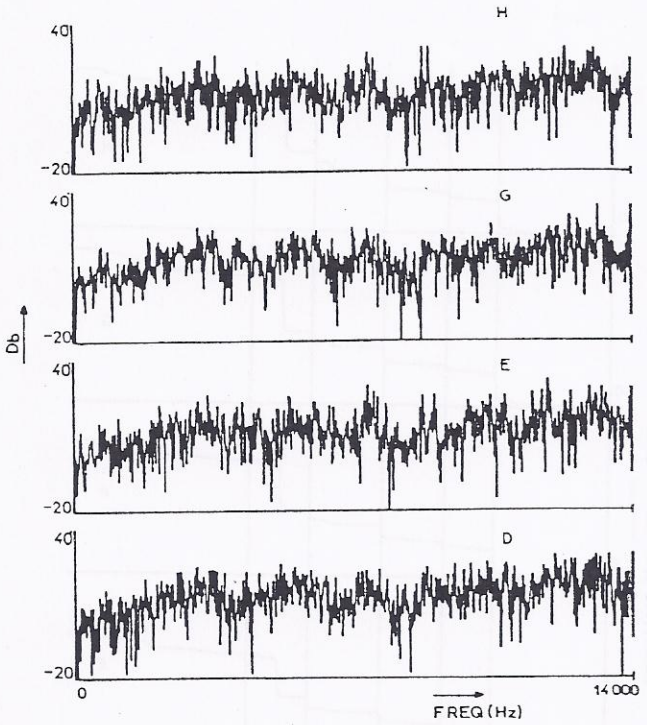

Fig. 11 Transfer function branch H2 for different operating points on the speedline at 9500 rpm

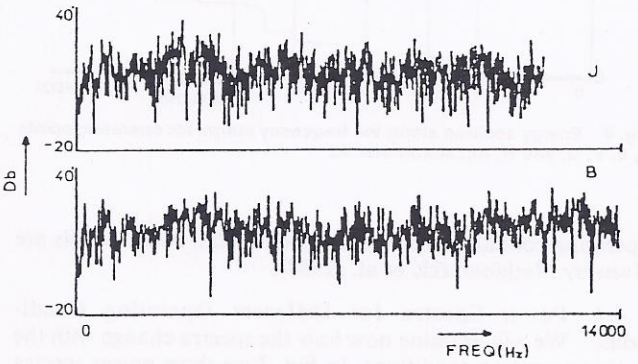

Fig. 12 Transfer function, branch H1, for 8500 rpm, 11,085 rpm

respectively. It is seen that between the 8500 rpm and 9500 rpm speedlines there is a lower degree of similarity, while between them and the 11,085 rpm the degree of similarity becomes even lower.

From the above discussion, we can conclude that the calculated transfer function is not fully independent of the operating point, but depends to some extent on the rotational speed and secondarily on the power level. A possible reason for this dependence is the change of temperatures associated with operation at different speeds. Changes of dimensions due to thermal expansion can, for example, reduce clearances between parts, and change the stiffness of the structure. Another possible reason is the bias errors due to our assumption about relations between the distributed inputs in lumping them. In reality the inputs taken into account are associated with the ones that are not, by nonlinear relations. Nonlinearities are expected to exist, mainly with respect to the operating point and aerodynamic excitations. Statistical reasons for this dependence are also present, due to errors resulting from noise in the inputs and the output. These errors decrease with the signal-to-noise ratio; therefore they are expected to be smaller

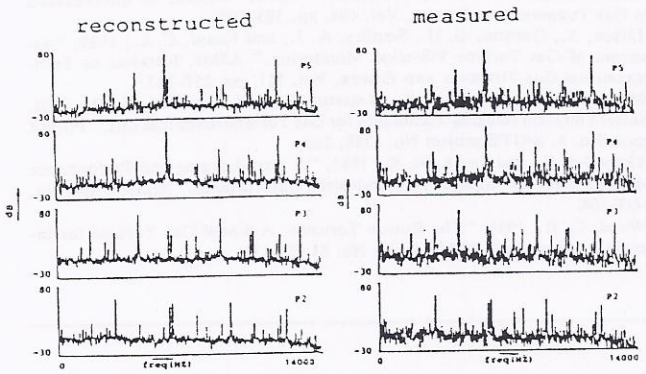

Fig. 13 Comparison between measured and reconstructed power spectra of pressure transducers

at the frequencies of the periodic components (peaks in the spectra) than at the frequencies of the broadband region.

6 Unsteady Pressure Signal Reconstruction

One of the purposes of the transfer function calculations is to enable the reconstruction of the casing excitations when the response is known. We present, now, how this is done.

The unsteady pressure signals of the first four stages' rotors have been reconstructed from the signals of accelerometers A1–A6 by employing the casing transfer function. The four unsteady pressure transducers P2–P5 have been regarded as outputs and the six accelerometers as inputs. This inverse direction modeling is a mathematical way devised to improve the accuracy of the calculations, by avoiding too many matrix inversions.

First the vector transfer functions $[H]$ are established, between each one of the unsteady pressure transducers P2–P5 (as output) and the six accelerometers A1–A6 (as inputs). The test data and relation (2) were used for this purpose. Then, using these transfer functions, the unsteady pressure transducer signal Fourier transforms are calculated. The Fourier transforms $[Y]$ of the pressure signals are calculated, from the transforms $[X]$ of the accelerometers, by means of the relation

$$[Y] = [H]\ [X] \tag{3}$$

Finally from the reconstructed Fourier transforms, the corresponding reconstructed spectral densities are calculated.

Using this procedure, the power spectra for the pressure transducers at the operating point F were reconstructed. The time domain signals of the accelerometers at that operating point were the inputs and a transfer function, resulting from an averaging of transfer functions at all operating points at that speed. A comparison with the corresponding directly calculated spectrum (Fig. 13) shows a very good agreement, particularly at frequencies corresponding to the periodic components of the signals.

The reason for the observed decrease in the level of the broadband random noise is probably the cross-multiplication averaging operations of the Fourier transforms in these frequencies. The corresponding Fourier transform values of the other unsteady pressure transducers or accelerometers involved in the calculation of cross-spectral densities are uncorrelated.

The same has been done for all the other available operating points. The general conclusion drawn is that for any operating point the spectral densities of unsteady pressure transducers P2–P5 can be satisfactorily reconstructed from the accelerometers' A1–A6 signals, using a complex average vector transfer function for the speedline of the operating point. This fact proves also rigorously the conclusion of the previous section, that transfer functions corresponding to different operating points of a speedline are similar. Thus, averaging over the different operating points does not influence the possibility of reconstructing features of the internal pressure signals.

Reconstruction of spectra at operating points on one speedline by using a transfer function evaluated at a different one was also attempted. The conclusion drawn is that, for any operating point, the reconstruction is not very successful when using an average transfer function from a different speedline. This fact confirms the conclusion of the previous section, that the transfer function similarity becomes weaker, when we change speedline. We can finally say that a single transfer function can be established for one rotational speed.

7 Conclusions

The experimental investigation reported above gives the possibility of drawing conclusions about the diagnostic value of the various measured quantities.

Unsteady pressure measurements can be used for identifying the operating condition of rotating blades. Such measurements are expected to provide a clear picture of blading faults.

Accelerometer measurements have the following features:

- The signals from accelerometers on the casing contain information about the operating conditions of compressor stages. Since the corresponding energy content is dominant along the frequency range, appropriate filtering should be employed, when shaft-related problems are considered.
- Each accelerometer signal carries information not only from the stage in its immediate vicinity, but also from other stages along the compressor.
- The vibrations of the compressor casing surface are not symmetrically distributed around the circumference. This fact is of diagnostic value, since accelerometers placed at the same axial location can provide information about stages at other axial locations.

Concerning the casing transfer characteristics:

- Transfer functions have been established, in order to relate pressure transducer outputs to those of accelerometers.
- Transfer functions from operating points at a certain speedline are similar, while transfer functions for different speeds show a smaller degree of similarity.

Using transfer functions, the power spectra of pressure transducers have been reconstructed using the accelerometer signals as inputs. It was shown that the reconstruction is successful by using one single transfer function for one rotational speed.

These last conclusions prove that: By following appropriate techniques, such as the ones we applied, it is possible to deduce information about phenomena at the engine interior, from measurements on the casing. In principle, it seems that it will be possible to diagnose engine condition from such measurements.

Acknowledgments

The work reported in this paper has been carried out within the frame of research contract BRITE No. RI 1B-0159-F(CD). The authors express their thanks to the Hellenic General Secretariat for Research and Technology and the European Communities, for their financial support. Thanks are expressed to METRAVIB RDS and RUSTON GAS TURBINES, for providing the instrumentation and the test engine. The experiments were possible only by their cooperation. Special thanks are due to Mr. M. K. Smith for valuable discussions and suggestions and to Dr. P. Wetta for his excellent cooperation in preparing and executing the experiments.

References

Baines, N., 1987, *Modern Vibration Analysis in Condition Monitoring Noise and Vibration Control Worldwide*, May, pp. 148–151.

Barschdorff, D., and Korthauer, R., 1986, "Aspects of Failure Diagnosis on Rotating Parts of Turbomachines Using Computer Simulation and Pattern Rec-

ognition Methods," Paper No. H1, International Conference on Condition Monitoring, Brighton, United Kingdom, May 21–23.

Bendat, J. S., and Piersol, A. G., 1971, *Random Data: Analysis and Measurement Procedures*, Wiley-Interscience, New York.

Bently, D., Zimmer, S., Palmatier, G., and Muszynska, A., 1986, *Interpreting Vibration Information From Rotating Machinery. Noise and Vibration Control Worldwide*, Part I, June, pp. 174–176; Part 2, July.

Carchedi, F., and Wood, G. R., 1982, "Design and Development of a 12:1 Pressure Ratio Compressor for the Ruston 6-MW Gas Turbine," ASME Journal of Engineering for Power, Vol. 104, pp. 823–831.

Laws, W., and Muszynska, A., 1987, "Periodic and Continuous Vibration Monitoring for Preventive/Predictive Maintenance of Rotating Machinery," ASME Journal of Engineering for Gas Turbines and Power, Vol. 109, pp. 159–167.

Lifshits, A., Simmons, H., and Smalley, A., 1986, "More Comprehensive Vibration Limits for Rotating Machinery," ASME Journal of Engineering for Gas Turbines and Power, Vol. 108, pp. 583–590.

Lifson, A., Quentin, G. H., Smalley, A. J., and Knauf, C. L., 1989, "Assessment of Gas Turbine Vibration Monitoring," ASME Journal of Engineering for Gas Turbines and Power, Vol. 111, pp. 257–263.

Mathioudakis, K., Loukis, E., Stamatis, A., and Papailiou, K. D., 1988, "Noise/Vibration Imaging Techniques for Gas Turbine Investigations," Project Report No. 3, BRITE project No. 1368, June.

Timperley, S., and Smith, M. K., 1983, "A Data-Logging and Performance Analysis System for Application to Industrial Gas Turbines," ASME Paper No. 83-GT-104.

Wood, G. R., 1981, "The Ruston Tornado. A 6-MW Gas Turbine for Industrial Application," ASME Paper No. 81-GT-171.

(Contents continued)